*Acta Cryst.* (1997). **B53**, 241–251

# Conformational Analysis of Macrocyclic Ether Ligands. I. 1,4,7,10-Tetraoxacyclododecane and 1,4,7,10-Tetrathiacyclododecane

P. R. RAITHBY,[a]* G. P. SHIELDS[a] AND F. H. ALLEN[b]

[a]*Department of Chemistry, Lensfield Road, Cambridge CB2 1EW, England, and* [b]*Cambridge Crystallographic Data Centre, 12 Union Road, Cambridge CB2 1EZ, England. E-mail: prrl@cam.ac.uk*

(*Received 27 August 1996; accepted 4 November 1996*)

## Abstract

Crystallographic results retrieved from the Cambridge Structural Database (CSD) have been used to perform systematic conformational analyses of both free and metal-coordinated unsaturated 12-membered oxa and thia macrocycles. Conformational classifications established using symmetry-modified Jarvis–Patrick clustering are visualized in conformational space by principal component analysis (PCA) plots. These show that the relationship between cluster populations and relative molecular mechanics energies is modified by the coordination requirements of a metal ion. With oxa donors the [3333] conformer (oxygen in edge positions) predominates for metal-coordinated macrocycles, with the donor atoms in a square-planar arrangement, whilst the [48] conformer occurs bound in a *cis*-octahedral fashion to metal ions and the [66] conformer does not bind in an *endo*-dentate manner at all. The [3333] and [66] conformers are both common for free ligands, reflecting their similar molecular mechanics energies; the conformation is often determined by the hydrogen-bonding network. There are few thia examples: it is found that conformers with low molecular mechanics energies are unsuited to metal coordination and substantial reorganization is necessary for chelation. The differences in behaviour of oxa and thia macrocycles may be rationalized in terms of differing torsion-angle preferences for C*X*CC and *X*CC*X* units (*X* = O, S).

## 1. Introduction

A key area of coordination chemistry that has developed over the last two decades is that of molecular recognition (Cram, 1988; Lehn, 1988; Pedersen, 1988). Work in this area has centred on the design of ligands which have been tailored to coordinate preferentially with specific metal ions (Lindoy, 1989). The ligands that have been used to achieve this aim have often been macrocyclic and it has been found in many cases that the conformation of the macrocycle is important in determining whether or not the required 'recognition' is achieved; the conformation of the coordinated macrocycle is often different to that observed for the free ring. An understanding of the factors which determine the configuration adopted by a particular macrocycle with a specific metal ion may be gained by a systematic analysis of the structures observed for the whole range of macrocyclic coordination complexes. This information is readily available in the Cambridge Structural Database (CSD; Allen *et al.*, 1991).

Several studies using molecular mechanics methodologies (Blake, Gould, Halcrow & Schröder, 1993; Hay, Rustad & Hostetler, 1993; Lockhart *et al.*, 1992; Setzer, Tang, Grant & Van Derveer, 1991) and conformational mapping (Fyles & Gandour, 1992) have been applied to metal macrocycle complexes with crystallographic coordinates from the CSD taken as the starting point for the calculations. In particular, a comprehensive conformational study of the macrocycle 1,4,7-trithiacyclononane in metal complexes (Beech, Cragg & Drew, 1994) has been performed and the majority of crystal structures containing [9]ane$S_3$ with a variety of metals were modelled successfully. However, in this study it proved necessary to estimate the ideal *M*—S bond length as the standard force-field was inappropriate.

The problem of including metals in molecular mechanics calculations has not been fully resolved and an alternative methodology using analytical techniques based on trends observed in a large number of individual crystal structures has been developed. This methodology has already been applied to carbon-containing ring systems. The methods of clustering and principal component analysis (PCA: Murray-Rust & Bland, 1978; Chatfield & Collins, 1980; Auf der Heyde, 1990) were used, with structural data taken from the CSD. Successful analyses have already been performed on the conformations adopted by carbocyclic (Allen, Doyle & Taylor, 1991*a*,*b*; Allen & Taylor, 1991; Allen, Doyle & Auf der Heyde, 1991; Allen, Howard & Pitchford, 1993) and heterocyclic (Allen, Doyle & Taylor, 1991*c*; Allen & Fortier, 1993) unsaturated rings containing 4–7 atoms.

In this paper we extend the methodology used to analyse the conformations adopted by 1,4,7,10-tetraoxacyclododecane and 1,4,7,10-tetrathiacyclododecane and their derivatives in both free macrocycles

ISSN 0108-7681 © 1997

Table 1. *CSD refcodes for retrieved data sets*

(1), (2) and (3) and derivatives

BARVOF
BEYHES
BIWFUI
CEMVIZ
CEVMUL
CEVNAS
CIJWIB
CLCOPB10
CUXXIC
CUXXOI
DAZWOQ
DEKNUC
DUGYUZ
DUWYOJ
FALGAA
FEZXIR
FOPCAO01
FOPPOP
FOPPUV
FORZOB
FUYDEI
GARLIU10
GETSED
GIMWII
GINNUM
GINPAU
GINPEY
GINPIC
GINPOI
GINPUO
GINRAW
GINREA
GINRIE
GINROK
GIPCOX
HARDAF
JOJNOL
JOJROP
JORLIL
JUWHIS
JUWHOY
KAMWIE
KAMZON
KAYGUM
KEVRAE
KOBHUE
KOKLOL
KORKOR
KUNMEL
LAGJEI
LAGJOS
LEBKIM
LEFGEI
PEZPIT
PIBVUR
PITVET
SELFIY
SISMUC
SISNAJ
SISNEN
SODGAT
SOMWAS
SUBREM
SUGKAG
SUMSUO
TOXCDO
TOXCDP
TOXDMG
TOXDOD
TXCDCU
TXCDNA
TXDCUN11
VEGSIJ10
VEJNED
VEWYEB
VITJUD
VITKAK
VOKDEE
VOSJIW
VOSTEC
WAKFUJ
WEKHEZ
YAHJUM
YATBIE
YUKHIV

Cyclododecane and derivatives

CDODEC
DPXCYD
HDODPO
HPXCDP
JIHZIJ
LESSEH

and their coordination complexes, and compare the results with those obtained from molecular mechanics calculations for the free macrocycles.

## 2. Methodology

Version 5.09 (April 1995, 146 232 entries) of the Cambridge Structural Database (CSD) was used throughout. The programs *QUEST3D*, *GSTAT* and *VISTA* (Cambridge Structural Database, 1992, 1994, 1995) were employed for the substructure search, information retrieval and data analysis.

Initial substructure searches located the required macrocycles (1), (2) and (3) (Fig. 1) and their substituted derivatives. The O or S atoms and C atoms (constrained to have a total coordination number of four, *i.e.* $sp^3$ hybridized) were defined as being singly bonded in the search query. Secondary search criteria were used to select only those entries (*a*) with $R \leq 0.10$, (*b*) error-free at the 0.02 Å level and (*c*) with average e.s.d. of the C—C bonds less than 0.03 Å or not specified. Entries with disorder reported in the macrocyclic ring (but not in any other part of the structure) were rejected after manual inspection. The retained CSD refcodes are reported in Table 1 and full literature citations have been deposited as supplementary material.*

Conformational clustering was performed using the program *GSTAT* (Murray-Rust & Raftery, 1985*a*,*b*). Cluster analysis was based on the intra-annular torsion angles and the Jarvis–Patrick (Jarvis & Patrick, 1973) algorithm, as modified by Allen, Doyle & Taylor (1991*b*) to take into account the permutational isomerism of the fragments. The data set was expanded to fill the topological symmetry space by use of bond permutational symmetry operators and the inversion operator (which reverses the sign of every torsion angle). The Jarvis–Patrick procedure employs four user-defined variables: (i) a power factor (PWR) defining the metric to be used in dissimilarity calculations, where PWR = 1 corresponds to the 'city-block' metric and PWR = 2 to the Euclidean metric; (ii) $K_{NN}$, the maximum length of the nearest-neighbour list for each fragment

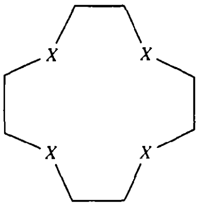
(1*a*) *X*=O; (1*b*) *X*=S

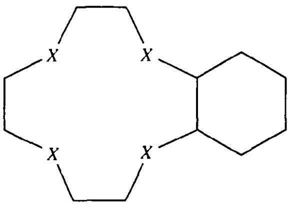
(2*a*) *X*=O; (2*b*) *X*=S

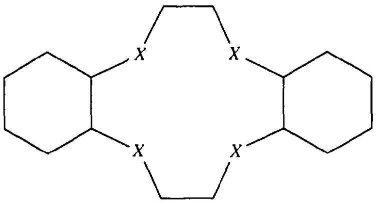
(3*a*) *X*=O; (3*b*) *X*=S

Atom permutational operators:

1 2 3 4 5 6 7 8 9 10 11 12
4 5 6 7 8 9 10 11 12 1 2 3
7 8 9 10 11 12 1 2 3 4 5 6
10 11 12 1 2 3 4 5 6 7 8 9
4 3 2 1 12 11 10 9 8 7 6 5
7 6 5 4 3 2 1 12 11 10 9 8
10 9 8 7 6 5 4 3 2 1 12 11
1 12 11 10 9 8 7 6 5 4 3 2

Bond permutational operators:

1 2 3 4 5 6 7 8 9 10 11 12
4 5 6 7 8 9 10 11 12 1 2 3
7 8 9 10 11 12 1 2 3 4 5 6
10 11 12 1 2 3 4 5 6 7 8 9
3 2 1 12 11 10 9 8 7 6 5 4
6 5 4 3 2 1 12 11 10 9 8 7
9 8 7 6 5 4 3 2 1 12 11 10
12 11 10 9 8 7 6 5 4 3 2 1

Fig. 1. Chemical substructures (1), (2) and (3).

---

* A list of CSD refcodes has been deposited with the IUCr (Reference: HA0151). Copies may be obtained through The Managing Editor, International Union of Crystallography, 5 Abbey Square, Chester CH1 2HU, England.

($p$); (iii) $K_{\rm JP}$, the Jarvis–Patrick clustering criterion, *i.e.* the number of fragments which must be common to the nearest-neighbour lists of fragments $p_1$ and $p_2$, such that both fragments may be assigned to the same cluster; (iv) $D_{\rm max}$, a maximum dissimilarity above which pairs of fragments may not be nearest neighbours, even if the $K_{\rm NN}$ limit is not exceeded. The values of the user-defined variables were adjusted manually until a chemically reasonable set of conformational clusters was obtained. A symmetry-expanded list of torsion angles was generated in *GSTAT* and imported into *VISTA* for further statistical calculations and principal component analysis (PCA).

Molecular mechanics calculations were performed using a modified MM2 force field (Allinger, 1977; Allinger & Yuh, 1981), as implemented in the program *MacroModel* (Mohamadi *et al.*, 1990; Columbia University, 1994). Calculations were performed on the free ligands alone with explicit lone pairs on oxygen donor atoms. The initial structures for minimization were imported from the CSD if suitable examples existed; otherwise, the conformation was selected by the temporary imposition of appropriate torsional constraints. Fragments with different donor atoms were generated simply by changing the atom type and allowing bond distances to relax in the minimization. No attempt was made to model the behaviour of metal-coordinated species directly.

The conformers are designated in the shorthand notation of Dale (1963, 1973): two successive *gauche* torsion angles of the same sign are taken to constitute a corner and the number of bonds between corners are listed successively between square brackets. The starting point and direction followed around the ring are chosen so as to give the smallest overall number. Two successive *gauche* torsion angles of opposite signs constitute a pseudo-corner and are neglected in this treatment. Where conformers have the same torsional sequence, but different positions of the hetero-atoms, they are distinguished by alphabetical suffixes.

## 3. Results

The presence of hetero-atoms in the 12-membered ring (1) (Fig. 1) reduces its topological symmetry from the $D_{12h}$ of the parent cycloalkane to the more tractable $D_{4h}$. The 12 torsion angles (Fig. 2) span the representations $3E_g \oplus 2A_{1u} \oplus A_{2u} \oplus 2B_{1u} \oplus B_{2u}$ and appropriate symmetry-adapted linear combinations are given in Table 2. $D_{4h}$ symmetry can only be realized in real space by a planar ring and three of the symmetry coordinates do not describe feasible infinitesimal displacements from this geometry. For real deformations in chemically reasonable rings these coordinates are formally redundant in the sense that they can be derived geometrically given the $(n - 1)$ bond lengths, $(n - 2)$ angles and $(n - 3)$ torsion angles necessary to describe the fragment fully. However, the geometric manipulation involved is far from trivial and it is more useful to quote 12 torsion angles or linear combinations.

Table 2. *Symmetry-adapted deformation coordinates for (1)*

| | IR | Kernel | Cokernel* | Coordinate |
|---|---|---|---|---|
| S1*a* | $E_g$ | $C_i$ | $C_{2h}$ | $\frac{1}{2}(\tau_1 + \tau_3 - \tau_7 - \tau_9)$ |
| S1*b* | $E_g$ | $C_i$ | $C_{2h}$ | $\frac{1}{2}(\tau_4 + \tau_6 - \tau_{10} - \tau_{12})$ |
| S2*a* | $E_g$ | $C_i$ | $C_{2h}$ | $\frac{1}{2}(\tau_1 - \tau_3 - \tau_7 + \tau_9)$ |
| S2*b* | $E_g$ | $C_i$ | $C_{2h}$ | $\frac{1}{2}(\tau_4 - \tau_6 - \tau_{10} + \tau_{12})$ |
| S3*a* | $E_g$ | $C_i$ | — | $1/2^{1/2}(\tau_2 - \tau_8)$ |
| S3*b* | $E_g$ | $C_i$ | — | $1/2^{1/2}(\tau_5 - \tau_{11})$ |
| S4 | $A_{1u}$ | $D_4$ | — | $1/8^{1/2}(\tau_1 + \tau_3 + \tau_4 + \tau_6 + \tau_7 + \tau_9 + \tau_{10} + \tau_{12})$ |
| S5 | $A_{1u}$ | $D_4$ | — | $\frac{1}{2}(\tau_2 + \tau_5 + \tau_8 + \tau_{11})$ |
| S6 | $A_{2u}$ | $C_{4v}$ | — | $1/8^{1/2}(\tau_1 - \tau_3 + \tau_4 - \tau_6 + \tau_7 - \tau_9 + \tau_{10} - \tau_{12})$ |
| S7 | $B_{1u}$ | $D_{2d}$ | — | $1/8^{1/2}(\tau_1 + \tau_3 - \tau_4 - \tau_6 + \tau_7 + \tau_9 - \tau_{10} - \tau_{12})$ |
| S8 | $B_{1u}$ | $D_{2d}$ | — | $\frac{1}{2}(\tau_2 - \tau_5 + \tau_8 - \tau_{11})$ |
| S9 | $B_{2u}$ | $D_{2d}$ | — | $1/8^{1/2}(\tau_1 - \tau_3 - \tau_4 + \tau_6 + \tau_7 - \tau_9 - \tau_{10} + \tau_{12})$ |

* McDowell (1965).

The search yielded 85 hits comprising 139 fragments. Of these, 132 fragments contained O donor atoms (13 free, two $\eta^1$- and 117 $\eta^4$-coordinated) and seven S donor atoms (two free, one $\eta^2$-, one $\eta^3$- and three $\eta^4$-coordinated). The most reasonable set of clusters (Table 3) was obtained with $K_{\rm NN} = 15$, $K_{\rm JP} = 6$, $D_{\rm max} = 0.15$ and PWR = 1. Some difficulty was experienced in selecting a suitable value of $K_{\rm NN}$ as a consequence of the disparate sizes of the conformational clusters. Cluster (1) tended to split into two or more clusters if smaller values of $K_{\rm NN}$ were used, since this conformation exhibits a

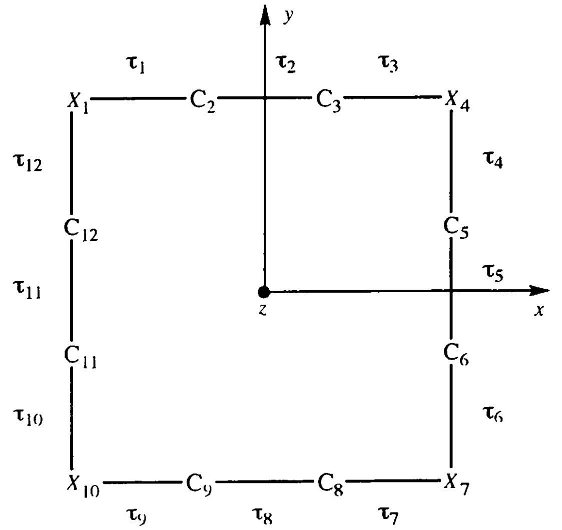

Fig. 2. Atomic and permutational symmetry groups for (1) ($X$ = O, S).

Table 3. *Cluster analysis results for fragments (1), (2) and (3) and torsion angles (°) of equivalent alkanes*

| Cluster | (1) | (3) | (4) | (6) | (2) | (5) |
|---|---|---|---|---|---|---|
| Size | 96 | 9 | 6 | 4 | 4 | 3 |
| Conformer | [3333]*B* | [66]*B* | [3333]*B* | [48] | [2334]*B* | [3333]*B* |
| Symmetry | $C_4$ | $C_i$ | $C_4$ | $C_s$ | $C_1$ | $C_4$ |
| Most representative fragment | FEZXIR(d) | SELFIY | YUKHIV | VOKDEE | JUWHOY | GIMWII(e)*<br>KORKOR(b)<br>PEZPIT |
| Mean or representative torsion angle sequence (°) | −164.7 (5) | 108.9 (30) | 154.8 (31) | 167.1 (25) | 162.7 (36) | −136.8 |
| | 56.9 (4) | −75.6 (13) | −47.5 (40) | −52.9 (34) | −45.5 (9) | 23.2 |
| | 82.5 (4) | 144.7 (43) | −90.8 (27) | −78.0 (27) | −71.7 (30) | 115.2 |
| | −164.7 (5) | −86.5 (20) | 154.8 (31) | 140.6 (41) | 160.5 (11) | −147.2 |
| | 56.9 (4) | −68.8 (19) | −47.5 (40) | −52.0 (17) | −52.4 (10) | 29.4 |
| | 82.5 (4) | 171.6 (46) | −90.8 (27) | −174.9 (66)† | −87.7 (37) | 99.1 |
| | −164.7 (5) | −108.9 (30) | 154.8 (31) | 174.9 (66)† | 177.2 (5) | −128.6 |
| | 56.9 (4) | 75.6 (13) | −47.5 (40) | 52.0 (17) | −52.0 (7) | 15.0 |
| | 82.5 (4) | −144.7 (43) | −90.8 (27) | −140.6 (41) | −96.7 (26) | 114.4 |
| | −164.7 (5) | 86.5 (20) | 154.8 (31) | 78.0 (27) | 86.7 (30) | −143.2 |
| | 56.9 (4) | 68.8 (19) | −47.5 (40) | 52.9 (34) | 44.9 (16) | 31.8 |
| | 82.5 (4) | −171.6 (46) | −90.8 (27) | −167.1 (25) | −175.5 (34) | 100.8 |

| Cluster | Singletons (17) | | | | | Alkanes |
|---|---|---|---|---|---|---|
| Size | 3 | 2 | 1 | 1 | 1 | 5 |
| Conformer | [48] | [3333]*A* | [2343] | [2334]*A* | [39] | [3333] |
| Symmetry | $C_s$ | $D_4$ | $C_1$ | $C_1$ | $C_1$ | $D_4$ |
| Most representative fragment | LEFGEI*<br>PITVET<br>VEGSIJ10(b) | FOPCAO01* | VOSTEC | KUNMEL | VEGSIJ10(a) | DPXCYD(a,*b)<br>HPXCDP(2)<br>JIHZIJ<br>LESSEH |
| Mean or representative torsion angle sequence (°) | −74.1 | −76.0 | −157.4 | 68.4 | −80.7 | 68.4 |
| | −58.1 | 173.8 | 65.1 | 48.8 | −62.6 | −160.5 |
| | 161.8 | −68.9 | 64.3 | −149.1 | −176.9 | 67.7 |
| | −159.9 | −70.2 | −166.2 | 57.8 | −70.7 | 69.4 |
| | 55.3 | 174.0 | 67.2 | 65.1 | −66.0 | −158.1 |
| | 78.0 | −74.1 | 70.7 | −179.4 | 148.9 | 68.6 |
| | −124.5 | −73.2 | −94.7 | 75.0 | −111.5 | 66.1 |
| | 54.5 | 173.1 | −56.8 | 77.8 | 65.4 | −164.0 |
| | −164.8 | −72.3 | 174.7 | −67.2 | −173.9 | 68.9 |
| | 163.4 | −71.0 | −50.6 | −57.1 | 163.1 | 69.0 |
| | −54.2 | 173.9 | −56.1 | 173.9 | −68.8 | −156.9 |
| | 123.4 | −71.6 | 136.4 | −167.7 | 126.3 | 69.2 |

* Representative torsion angle sequence. † The signs of these torsion angles are reversed in some fragments.

broad range of torsion angles. The choice of a smaller $K_{JP}/K_{NN}$ ratio (0.4) than would normally be employed allowed clustering of uncommon conformations with fewer than $K_{NN}/2$ nearest-neighbours, within the $D_{max}$ threshold, whilst preventing cluster (1) from splitting. The symmetry-expanded mean torsion angle sequence corresponds to the cluster centroid in the conformational-parameter space and may not necessarily represent a realizable geometry in real space. Ideal point-group symmetries correspond to the symmetry of the special position occupied by the final cluster centroid in the 12-dimensional parameter space. The most representative fragment (Table 3, Fig. 3) is that closest to the cluster centroid, the distance being determined according to the value of PWR.

Principal component analysis results are summarized in Table 4. The first two principal components describe more than 80% of the torsional variance. Conformational clusters are identified on the scatter plots (Fig. 4). $PC_1$ is equivalent to S6 and $PC_2$ is a linear out-of-phase combination of S4 and S5. Fragments with inversion symmetry (*e.g.* [66]*B* conformers) appear at the origin of the plot (Fig. 4*a*), since such symmetry is lost along both $A_{1u}$ and $A_{2u}$ coordinates (the [66]*B* fragment KOKLOL is somewhat distorted and thus is displaced from the origin in Fig. 4*a*). The [3333]*A* conformation has ideal $D_4$ symmetry and thus the only examples (FOPCAO01a,b) in the data set appear as outliers on the $PC_2$ axis.

Fragments with ideal $C_4$ symmetry ([3333]*B*) may show displacements along both $PC_1$ and $PC_2$ axes and four symmetry-related permutations of cluster (1) appear on diagonals of the plot. That the majority of fragments are found in cluster (1) explains why the first two principal components describe such a large proportion of the variance. Flatter [3333]*B* conformations approach a (120, 0, −120°)$_3$ torsion angle sequence and $C_{4v}$ symmetry and thus appear on a line between two symmetry-related [3333]*B* clusters intersecting the $PC_1$

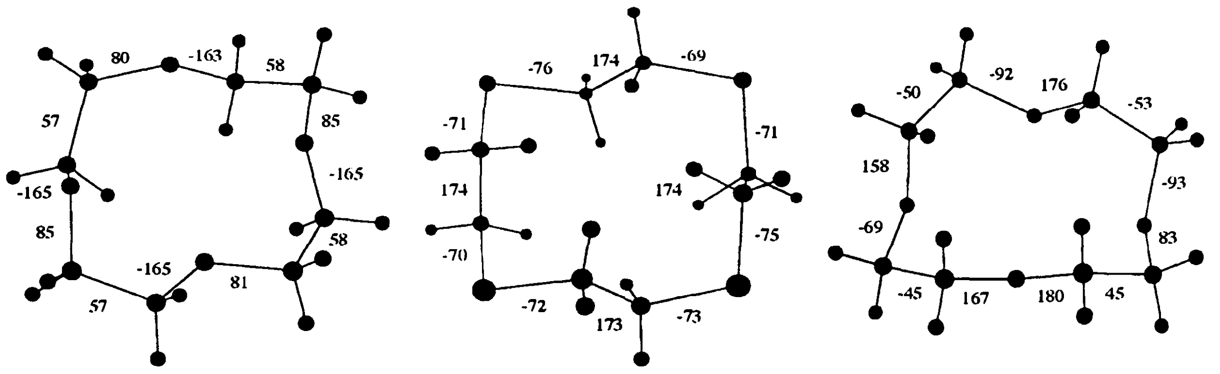

(1*a*) [3333]*B* FEZXIR(d) (1*b*) [3333]*A* FOPCAO01(a) (1*a*) [2334]*B* JUWHOY

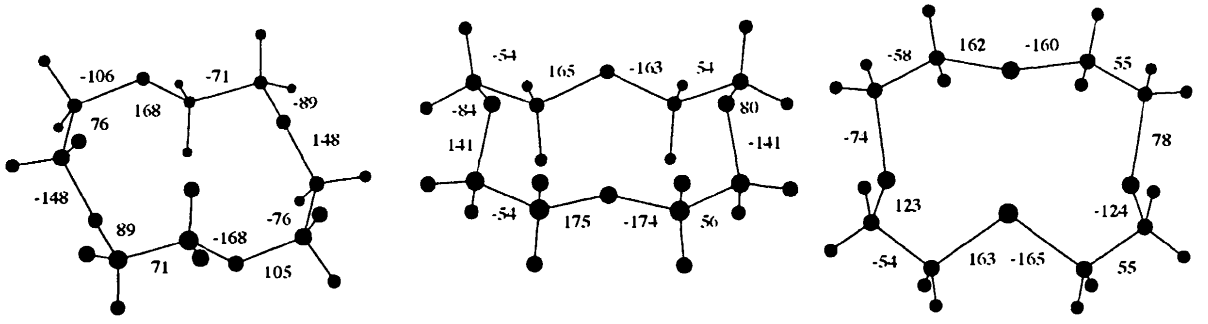

(1*a*) [66]*B* SELFIY (1*a*) [48] VOKDEE (1*b*) [48] LEFGEI

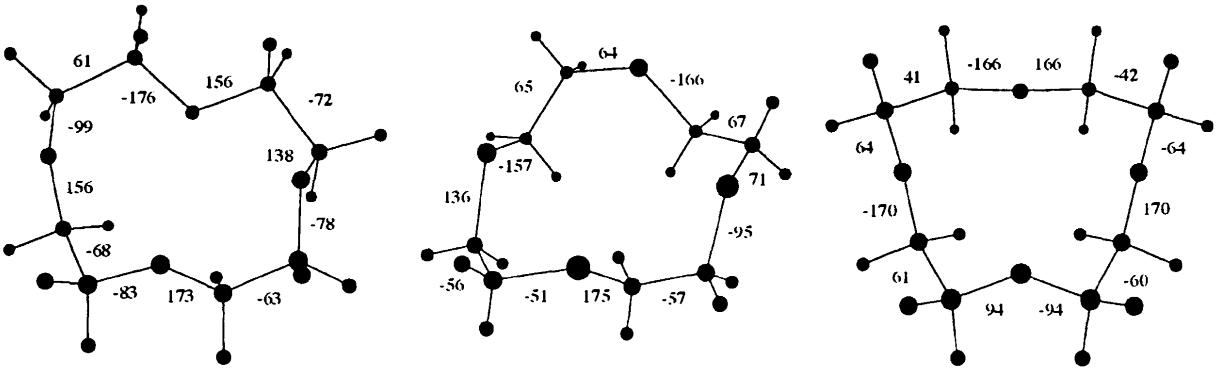

(1*a*) [39] MM2* (1*b*) [2343] VOSTEC (1*a*) [2343] MM2*

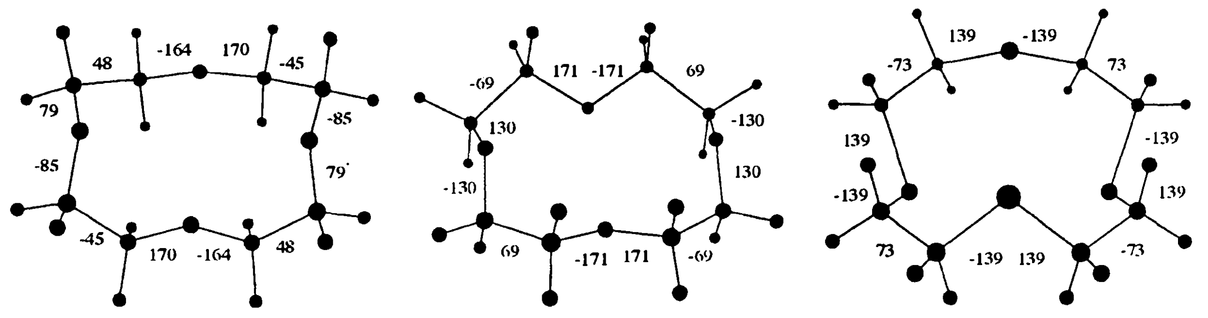

(1*a*) [2424] MM2* (1*a*) Anangular $C_{2v}$ MM2* (1*b*) Anangular $D_{2d}$ MM2*

Fig. 3. Perspective views of selected conformers of (1), (2) and (3) from CSD entries and molecular mechanics calculations with torsion angles (°).

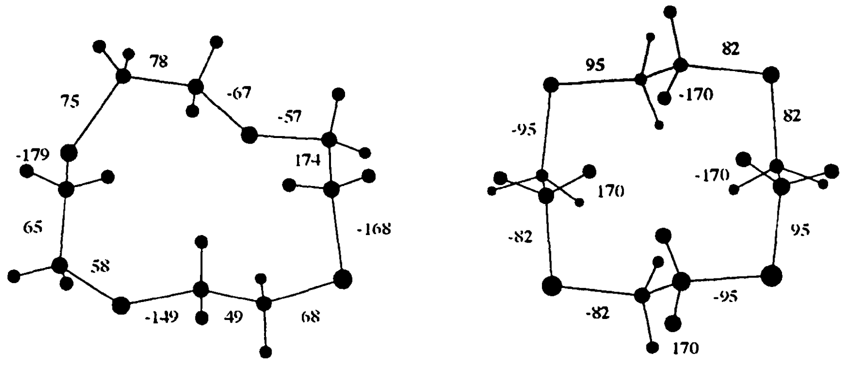

(1*b*) [2334]*A* KUNMEL (1*b*) [66]*A* MM2*

Fig. 3 (*cont.*)

axis; the distorted fragments can be described in terms of weighted disorder between two symmetry-related $C_4$ conformers. The [48] conformers appear displaced along the PC$_1$ axis, but not along PC$_2$, since only the former maintains mirror symmetry.

The degenerate principal components PC$_3$ and PC$_4$ together describe most of the variance of $E_g$ symmetry, a small proportion of the total since most fragments approach $C_4$ symmetry. The principal component axes PC$_3^*$ and PC$_4^*$ have been rotated by 15° about the origin with respect to PC$_3$ and PC$_4$, such that each maintains $C_{2h}$ cokernel (McDowell, 1965) symmetry (Fig. 4*c*). $C_1$ and $C_4$ conformers (without mirror or inversion symmetry) are distinguished more clearly in the scatter plot of PC$_1$ *versus* PC$_3^*$ (Fig. 4*b*). Fragments with $D_4$ symmetry ([3333]*A*) appear at the origin, $C_4$ ([3333]*B*) along the PC$_1$ axis and $C_i$ ([66]*B*) along PC$_3^*$. Mirror symmetry alone is conserved along a combination of $A_{2u}$ and $E_g$ cokernel coordinates; thus, $C_s$ and $C_1$ conformers in general appear off the axes in this plot and are clearly distinguished from 'flat' $C_4$ conformers in clusters (4) and (5) (Table 3). $B_{1u}$ and $B_{2u}$ deformations are relatively unimportant; these are only significant for conformers with $C_1$ symmetry (*e.g.* [2334] and [2343]). As a result, two principal component scatter plots are sufficient to represent the major conformational clusters visually in torsional space.

## 4. Discussion

The conformational preferences of the parent cyclododecane and higher cycloalkanes were discussed by Dale (1973). He suggested that even-membered rings with more than ten atoms would adopt quadrangular (*i.e.* having four corners) conformations with all-*anti* (*A*) torsion angles along the sides (as favoured for open-chain unbranched alkanes) and same-sign *gauche* (*G*) corners, the two sets of 1,4 CH···HC interactions essentially not being perturbed by one another in this arrangement. On the other hand, +*G*–*G* sequences lead to a formidable steric (1,5 pentane) interaction; +*G*–*G*+*G* and +*G*+*G*–*G*–*G* sequences are also accompanied by unfavourable (1,6 and 1,7, respectively) steric interactions, which may, however, be relieved by systematic deviations from ±60° torsion angles (Dale, 1973). In smaller rings ($\leq$ 15 atoms) other *trans*-annular interactions must also be considered.

Cyclododecane crystallizes in the space group *C*2/*m* and the molecules are statistically disordered over mirror planes (Dunitz & Shearer, 1960). This gives rise to an ambiguity in discerning the conformation, although it was suggested that a [3333] with crystallographic $C_2$ and approximate $D_4$ symmetry was the most likely of a number of models. A CSD search for simple 12-membered rings with coordinate data yielded four hits; all have the [3333] conformation with various substituents on the C$_{12}$ ring (torsion angle data given in Table 3). HDOPDO, for which coordinate data is not available, is also reported to have the same conformation (Samuel & Weiss, 1969).

The introduction of hetero-atoms modifies these conformational preferences (Zefirov, 1977; Uiterwijk, Harkema, van de Waal, Göbel & Nibbeling, 1983) and there is a marked difference in behaviour between oxygen and sulfur, primarily as a result of their size difference (Wolf, Hartman, Storey, Foxman & Cooper, 1987). Whereas *gauche* CCOC torsion angles are destabilized (Podo, Némethy, Indovina, Radics & Viti, 1974), since 1,4 H atoms are placed only 1.8 Å apart compared with the van der Waals separation of *ca* 2.4 Å, *gauche* CCSC angles are little destabilized, placing H atoms *ca* 2.4 Å apart (Fausto, Teixeira-Dias & Carey, 1987). Conversely, whilst *gauche* OCCO torsion angles are favoured (attractive *gauche* effect), *gauche* SCCS angles are disfavoured since the hetero-atom separation is such that attractive dispersion forces dominate for oxygen, whereas sulfur–sulfur interactions are repulsive due to the greater van der Waals radius (Cooper, 1988;

Table 4. *Principal component analysis of fragments (1), (2) and (3)*

| | $PC_1$ | $PC_2$ | $PC_3$ | $PC_4$ | $PC_5$ | $PC_6$ | $PC_7$ | $PC_8$ | $PC_9$ | $PC_{10}$ | $PC_{11}$ | $PC_{12}$ |
|---|---|---|---|---|---|---|---|---|---|---|---|---|
| Eigenvalue | 6.228 | 3.936 | 0.548 | 0.548 | 0.203 | 0.136 | 0.136 | 0.079 | 0.079 | 0.043 | 0.034 | 0.033 |
| % Variance | 51.90 | 32.80 | 4.56 | 4.56 | 1.69 | 1.13 | 1.13 | 0.66 | 0.66 | 0.35 | 0.28 | 0.27 |
| Symmetry | $A_{2u}$ | $A_{1u}$ | $E_g$ | $E_g$ | $B_{1u}$ | $E_g$ | $E_g$ | $E_g$ | $E_g$ | $A_{1u}$ | $B_{2u}$ | $B_{1u}$ |
| $\tau_1$ | 0.882 | 0.286 | 0.137 | 0.231 | 0.148 | 0.010 | 0.129 | 0.021 | 0.137 | 0.067 | 0.065 | 0.023 |
| $\tau_2$ | 0.000 | −0.905 | −0.311 | −0.181 | −0.082 | −0.124 | 0.138 | −0.021 | 0.022 | 0.042 | 0.000 | 0.084 |
| $\tau_3$ | −0.882 | 0.286 | 0.269 | 0.006 | 0.148 | −0.130 | 0.004 | −0.138 | −0.016 | 0.067 | −0.065 | 0.023 |
| $\tau_4$ | 0.882 | 0.286 | −0.231 | 0.137 | −0.148 | 0.129 | −0.010 | −0.137 | 0.021 | 0.067 | −0.065 | −0.023 |
| $\tau_5$ | 0.000 | −0.905 | 0.181 | −0.311 | 0.082 | 0.138 | 0.124 | −0.022 | −0.021 | 0.042 | 0.000 | −0.084 |
| $\tau_6$ | −0.882 | 0.286 | −0.006 | 0.269 | −0.148 | 0.004 | 0.130 | 0.016 | −0.138 | 0.067 | 0.065 | −0.023 |
| $\tau_7$ | 0.882 | 0.286 | −0.137 | −0.231 | 0.148 | −0.010 | −0.129 | −0.021 | −0.137 | 0.067 | 0.065 | 0.023 |
| $\tau_8$ | 0.000 | −0.905 | 0.311 | 0.181 | −0.082 | 0.124 | −0.138 | 0.021 | −0.022 | 0.042 | 0.000 | 0.084 |
| $\tau_9$ | −0.882 | 0.286 | −0.269 | −0.006 | 0.148 | 0.130 | −0.004 | 0.138 | 0.016 | 0.067 | −0.065 | 0.023 |
| $\tau_{10}$ | 0.882 | 0.286 | 0.231 | −0.137 | −0.148 | −0.129 | 0.010 | 0.137 | −0.021 | 0.067 | −0.065 | −0.023 |
| $\tau_{11}$ | 0.000 | −0.905 | −0.181 | 0.311 | 0.082 | −0.138 | −0.124 | 0.022 | 0.021 | 0.042 | 0.000 | −0.084 |
| $\tau_{12}$ | −0.882 | 0.286 | 0.006 | −0.269 | −0.148 | −0.004 | −0.130 | −0.016 | 0.138 | 0.067 | 0.065 | −0.023 |

Juaristi, 1979; Desper, Powell & Gellman, 1990). These factors reinforce each other, with the result that *gauche* $XCCX$ and *anti* $CCXC$ torsion angles are favoured with $X$ = O and the converse with $X$ = S (or Se) hetero-atoms in macrocycles with $(CH_2)_2$ units. The preference for +*G*+*G* over −*G*+*G* sequences is diminished where the corner atom is S, or particularly Se, since the distance between 1,5 H atoms is increased (Batchelor, Einstein, Gay, Gu & Pinto, 1991).

### 4.1. *1,4,7,10-Tetraoxacyclododecane and derivatives (1a, 2a and 3a)*

The molecular mechanics results for (1*a*) presented in Table 5 differ from those reported previously. Bovill, Chadwick, Sutherland & Watkin (1980) found the [3333]*B* conformation to be *ca* 7.5 kJ mol$^{-1}$ lower in energy than [66]*B* largely as a result of lower torsional strain. Our MM2* calculations give [66]*B* as the lower energy conformer due to more favourable electrostatic interactions. The difference may be ascribed to the absence of explicit lone pairs on O atoms (which were treated as spherical) in the force field used by Bovill, Chadwick, Sutherland & Watkin (1980). The crystal structures of free (1*a*) (TOXCDP), two stereoisomers of free (3*a*) (SISMUC, SIJNAJ) and the bicyclic KOKLOL all show the [66]*B* conformer. However, the molecular mechanics calculations actually suggest that the [39] conformer is slightly lower in energy than either [66]*B* or [3333]*B*. This (1*a*) conformer only occurs in VEGSIJ10, coordinated to a uranium centre in a monodentate fashion. It would seem that the molecular mechanics calculations are not sufficiently accurate to allow relative energies of the order of a few kJ mol$^{-1}$ to be predicted reliably. In solution it is likely that several of these, and other, conformers are present at room temperature and entropy considerations will also be important in determining their relative proportions.

The energy differences between the [3333]*B*, [66]*B* and [48] conformers are not highly significant (5 kJ mol$^{-1}$ or less), although the energy of [2334]*B* is somewhat greater (Table 5). Both [3333]*B* and [66]*B* conformers have four *anti* CCOC torsion angles, which is the maximum possible with a (pseudo-) quadrangular conformation (Wolf, Hartman, Storey, Foxman & Cooper, 1987; Willey, Lakin & Alcock, 1992). Thus, they necessarily have four unfavourable CCOC *gauche* torsion angles. The [66]*B* conformer has two −*G*+*G* sequences, leading to 1,5 H···O(lone pair) interactions, and consequently these torsion angles deviate substantially from ±60° in the crystal structure of the free ligand (Groth, 1978).

The majority of the fragments in the data set are (1*a*) and (3*a*) examples. The [3333]*B* conformation is dominant in metal-coordinated species, since it presents its four donor atoms on the same side and there is little reorganization energy penalty. With ideal $C_4$ symmetry the four O atoms are coplanar and this situation generally prevails even if crystallographic symmetry is lower; the cation may lie above the plane of the donor atoms if it is too large for the cavity. This coordination mode is suited to a variety of coordination environments, including five-coordinate square-based pyramidal [*e.g.* (1*a*)Li(N(SiMe$_3$)$_2$), CEMVIZ], seven-coordinate 4:3 [*e.g.* (1*a*)BiCl$_3$, KAMDIE; (1*a*)Co($\eta^1$-NO$_3$)($\eta^2$-NO$_3$), CLCOPB], nine-coordinate capped square-anti-prismatic {*e.g.* [(1*a*)-Tb/La(H$_2$O)$_5$]$^{3+}$, FOPPUV, GINNUM} and ten-coordinate geometries [*e.g.* FUYDEI (1*a*)$_2$Ba(NCS)$_2$] represented in clusters (1), (4) and (5). Eight-coordinate square anti-prismatic species exist in which a cation is either sandwiched between two macrocycles {*e.g.* [Li/Na/Ag(1*a*)$_2$]$^+$, CEMVUL, BEYHES, CIJWIB} or the coordination sphere is completed by four other ligands {*e.g.* [(1*a*)YCl$_2$(OH$_2$)(O(H)CH$_3$)]$^+$, GINROK; [(1*a*)Ca(OH$_2$)$_4$]$^{2+}$, TOXCDO; (1*a*)PrCl$_3$(O(H)CH$_3$), VEWYEB}. The larger potassium cation occurs in the ten-coordinate hetero-sandwich complex [(1*a*)K([18]aneO$_6$)]$^+$ (PEZPIT); the cation is displaced 2.13 Å from the (1*a*) ring, but only 1.28 Å from the

18-crown-6, indicating a considerable size mismatch with the smaller macrocycle.

There are two distinct sets of C atoms in the [3333]*B* conformation, designated as $C_\alpha$ (in a plane nearest to the plane of the oxygen donor atoms) and $C_\beta$; the $C_\beta$—$C_\alpha$—O angles are systematically larger than the $C_\alpha$—$C_\beta$—O angles in some complexes (Boer, Neuman, van Remoortere & Steiner, 1974; van Remoortere & Boer, 1974). Furthermore, the *gauche* COCC torsion angles show a systematic deviation from ±60° [typically ≥ 70°; cluster (1) mean 82.5 (4)°] in order to relieve the unfavourable 1,4 CH···HC interaction (Rogers, Rollins & Benning, 1988; Uiterwijk, Harkema, van de Waal, Göbel & Nibbeling, 1983). Clusters (4) and (5) (Table 3) are flatter versions of the [3333]*B* conformation and several singletons are distorted variants. The existence of such structures may be an artefact of unresolved static or dynamic disorder between two mirror-image conformations in the crystal rather than a real flattening effect in some cases.

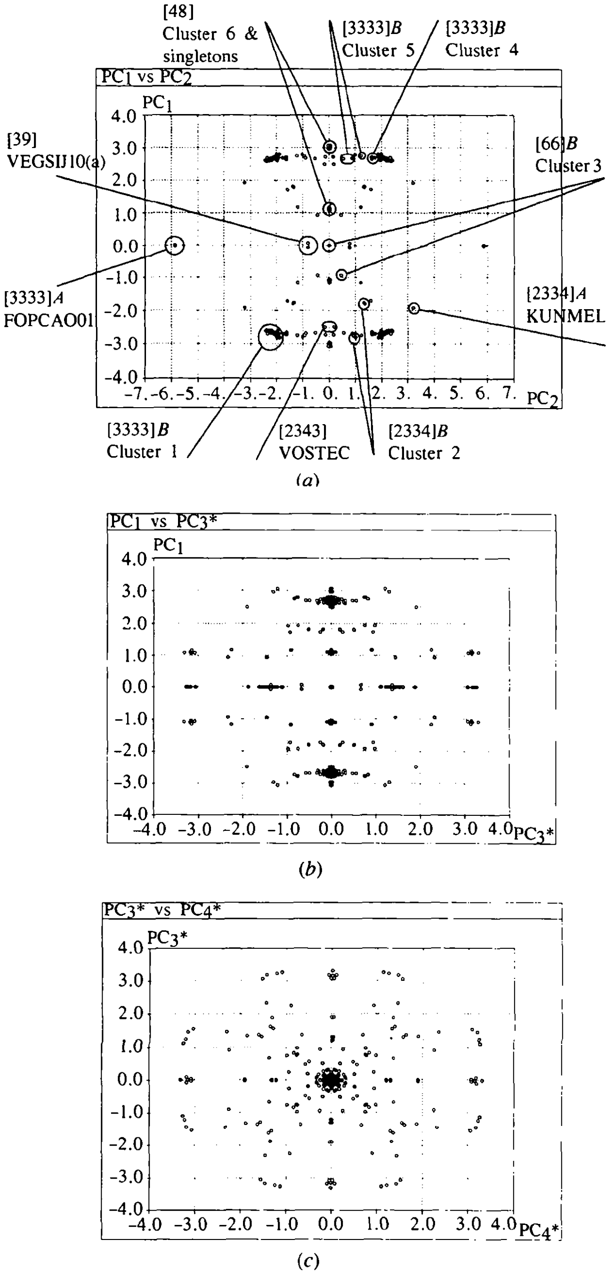

(*a*) (*b*) (*c*)

Fig. 4. Scatter plots of principal component scores for fragment (1), (2) and (3).

Table 5. *Relative molecular mechanics energies of free (1a) and (1b) conformations*

| Conformation | Ideal symmetry | MM2* energy (kJ mol$^{-1}$) (1*a*) | (1*b*) |
|---|---|---|---|
| [3333]*B* | $C_4$ | 4.4 | 8.1 |
| [3333]*A* | $D_4$ | 81.9 | 0.0 |
| [66]*B* | $C_i$ | 0.0 | 22.2 |
| [66]*A* | $C_{2h}$ | 83.0 | 10.8 |
| [2334]*A* | $C_1$ | — | 15.8 |
| [2334]*B* | $C_1$ | 13.1 | 16.8 |
| [2343] | $C_s$ | 18.8 | 20.3 |
| [2343] | $C_1$ | † | 19.8 |
| [48] | $C_s$ | 2.0 | 25.3 |
| [39] | $C_1$ | −1.5 | 17.5 |
| [2424] | $C_{2v}$ | 30.3 | 28.8 |
| Anangular | $C_{2v}$ | 15.1 | ‡ |
| Anangular | $D_{2d}$ | 17.6 | 40.5 |

† Conformer unstable - distorts to $C_s$ [2343]. ‡ Conformer unstable - distorts to $D_{2d}$ anangular.

The more distorted [2334]*B* conformation (Table 3) is formally derived from the [3333]*B* by the rotation of three adjacent torsion angles, *viz*. *A*→+*G*, –*G*→+*G* and –*G*→*A*, or alternatively from [48] by rotating two *anti* torsion angles to *gauche* and one +*G* torsion angle to –*G*; thus, it may be considered as intermediate between the [48] '*cis*' and [3333]*B* conformations. The [2334]*B* occurs when the coordination geometry dictates a less planar arrangement of the four O atoms as in the nine-coordinate $(1a)_2E$(NCMe) complexes [where *E* = Sb (JUWHIS) or *E* = Bi (JUWHOY)] and the ten-coordinate $(1a)\mathrm{Ln^{III}(NO_3)_3}$ species [where Ln = Eu (BIWFUI) or Ln = Y (Rogers & Kurihara, 1986)]. However, the ligand in $(2a)\mathrm{Eu^{III}(NO_3)_3}$ KAGYUM has the more common [3333]*B* conformation, suggesting that conformational preferences in such high coordination environments are not well defined and are dependent on macrocycle substituents and intermolecular forces. The [2334]*B* conformation is also adopted by the macrocycle in SISNEN (3*a*)Li(NCS), since the geometrical isomer of the ligand precludes [3333]*B* (the cyclohexane rings must be *exo* to the macrocycle in a metal complex) and this results in a more distorted square-based pyramidal lithium coordination geometry.

The [3333]*B* conformation is not suited to forming six-coordinate metal complexes, since one face is severely hindered by the $CH_2$ groups of the backbone and the lone pairs would not be oriented appropriately (van Remoortere, Boer & Steiner, 1975). Instead, the [48] $C_s$ conformation is usually adopted with the other ligands disposed in a *cis* manner [*e.g.* (1*a*)$Cu^{II}Cl_2$, TXCDCU]. This gives a severely distorted octahedral geometry since the $(CH_2)_2$ units are insufficiently long or flexible to bind to an octahedral metal centre with ideal *trans*-axial [135.2 (1)°] in TXCDCU] or equatorial bond angles. The axial Cu—O distances [2.343 (4) and 2.403 (3) Å] are significantly longer than the equatorial distances [2.113 (3) and 2.128 (3) Å], as would be expected for a $d^9$ tetragonally elongated $Cu^{II}$ ion. The [48] conformation is also found in the seven-coordinate complex $Ti_2(\mu_2\text{-}O)_2Cl_2(1a)_2$, SUBREM. The titanium coordination polyhedron could be described as a distorted pentagonal bipyramid with three ether donors in equatorial positions and the other in an axial site. The *trans*-axial angle of 166.8 (1)° and the axial–equatorial O(ether)MO(ether) angles are smaller than ideal, reflecting the limited flexibility of $(CH_2)_2$ chains between the donor atoms. However, the [48] conformer does allow a more ideal coordination polyhedron than would be achieved with [3333]*B*, given the fairly rigid geometry of the $Ti(\mu_2\text{-}O)_2Ti$ bridging unit.

The CSD entry WEKHEZ is of particular interest, since it contains the six-coordinate $(1a)Li(\eta^2\text{-}OS(Me)({=}O)NS(Me)({=}O)O)$ complex with both [48] and [3333]*B* conformations in the same crystal structure. The MM2* energies of the free ligands are comparable and the co-occurrence of these coordination isomers in the crystal suggests that the strain energy of the complexed macrocycle, the strength of the Li—O bonding and mutual repulsion of the ligand donor atoms are finely balanced. The coordination polyhedron with the [3333] ligand can be described as a cube with two vertices, related by a face-diagonal, removed (Blaschette, Nagel & Jones, 1994), whilst that with the [48] ligand is similar to TXCDCU, although the absence of a stereoelectronic tendency for tetragonal elongation allows a more ideal *trans*-axial angle [146.5 (2)°] to be achieved.

Krotz, Kuo & Barton (1993) and van Remoortere, Boer & Steiner (1975) have discussed why the $C_s$ *cis* conformation rather than either of the two possible $C_{2v}$ *cis* conformers (Fig. 3) is adopted with different heteroatoms ([48] $C_s$ being composed of one half of each $C_{2v}$ conformer). Molecular mechanics calculations on the oxa derivatives (Table 5) show both the [2424] (with all donor atoms directed to the same side) and the anangular (four pseudo-corners instead of corners and donor atoms directed up–down–up–down) conformers to be significantly higher in energy than [48]. The [2424] conformer has more bond-angle strain and less favourable electrostatic terms; its symmetry is reduced to $C_2$ in order to relieve short (2.06 Å) *trans*-annular CH···HC interactions. The anangular $C_{2v}$ has appreciable torsional strain (four COCC torsion angles of 129.5°) and two short (2.07 Å) *exo* CH···HC contacts as in the aza analogue (Krotz, Kuo & Barton, 1993). The more symmetrical $D_{2d}$ anangular conformer has slightly higher energy and ±68.7° OCCO and ±150.3° COCC torsion angles.

The [66]*B* conformation is not well suited to *endo*-dentate metal coordination, since its donor atoms are directed in pairs above and below the ring, although they are precisely coplanar. It occurs coordinated in an *exo*-dentate manner in the 2:1 complex $(1a)(AlCl_3)_2$ (DEKNUC). Both the [3333]*B* and [66]*B* conformers also occur in the secondary coordination sphere of the metal ions, hydrogen-bonded to solvent or coordinated water molecules. The conformation adopted is dictated by the nature of the hydrogen-bonding network, [3333] presenting four donor atoms on the same side and [66] two donors on each (GIPCOX, SODGAT, SUGKAG, TOXDMG, TXDCUN11). A similar hydrogen-bonding network is present in the co-crystal of [66]*B* (1*a*) with $(HO)Si(Ph)_3$, SELFIY, in which the macrocycle lies on an inversion centre and is hydrogen bonded to two symmetry-related silanol molecules.

### 4.2. *1,4,7,10-Tetrathiacyclododecane and derivatives (1b, 2b and 3b)*

Sulfur examples are less common, comprising only seven fragments in the data set. The free ligand adopts the [3333]*A* conformation with S atoms at the corners of the quadrangle in the solid state (FOPCAO, FOPCAO01). This has eight favourable *gauche* CCSC and four *anti* SCCS torsion angles and was the lowest energy conformer found in the molecular mechanics minimizations (Table 5). The [66]*A* conformer with S atoms at the corners has a substantially higher energy due to 1,5 pentane interactions about *–G+G* torsion angle sequences, despite the greater size of the S donor atom (Robinson & Sangokoya, 1988).

Substantial re-organization is required to convert the [3333]*A* to the [3333]*B* conformer. Four CCSC torsion angles must be rotated from *gauche* to *anti* placements and four SCCS torsion angles from *anti* to *gauche* (Willey, Lakin & Alcock, 1992) and this process is energetically unfavourable (Table 5); the ligand is not 'pre-organized' for *endo*-dentate complexation to metal centres, unlike the smaller 1,4,7-trithiacyclononane ligand (Blake & Schröder, 1990; Beech, Cragg & Drew, 1994). One fragment in cluster (1) has the [3333]*B* conformation, the four-coordinate $[Pt(1b)]^{2+}$ complex PIBVUR, with crystallographic $C_4$ symmetry, in which the Pt ion lies 0.33 Å above the (exact) sulfur donor atom plane. The [3333]*B* conformer is also present in the Pd analogue (Blake & Schröder, 1990) and a disordered $Cu^{II}$ structure (Pett *et al.*, 1983; Marsh, 1986).

Watzky, Waknine, Heeg, Endicott & Ochrymowyzc (1993) used molecular mechanics techniques to investigate complexes of Pt with a range of tetra-thia macrocycles [$n$]ane$S_4$, where $n = 12$–16. Whilst their calculations included only limited metal–sulfur stretching and bending terms and did not completely account for 'electronic' directional orbital-overlap effects at the metal centre (although it was indicated that they might account for up to 20% of the total energy), the calculations indicated that the total 'steric' energy was virtually independent of the size of the macrocycle. This may be attributed to the conflicting preferences of large metal ions for five- rather than six-membered chelate rings (Hancock, 1990) and larger hole sizes (Pett *et al.*, 1983).

The other S donor examples appear as singletons. Both LEFGEI (Rh) and PITVET (Ni) contain *cis*-octahedral $L_2M(1b)$ fragments with the [48] conformation, similar to the (1*a*) examples in cluster (6). Krotz, Kuo & Barton (1993) suggested that a folded *cis* geometry was adopted rather than *trans* because the cavity in the planar [3333]*B* conformer is too small. Whilst the ligand is not ideally suited to co-planar coordination of transition metals, steric hindrance from the $CH_2$ units in the axial site on the 'underside' of the ligand (van Remoortere & Boer, 1974; van Remoortere, Boer & Steiner, 1975) may be a more significant factor, disfavouring the *trans*-octahedral geometry. *trans*-Axial SMS angles are closer to the ideal value than in the (1*a*) analogues, a result of longer hetero-atom–carbon bond lengths, but still deviate substantially from 180° [166.14 (9)°, $M$ = Ni; 168.5 (1)°, $M$ = Rh].

The free [48] (1*b*) conformer is significantly higher in energy than either the [3333]*A* or the [3333]*B* conformers as a result of less favourable van der Waals repulsion and, especially, torsion angle terms (two CSCC torsion angles approach eclipsed placements). However, 1,4 S$\cdots$S interactions are reduced in the complex as electron density is donated from the S atoms to the metal. The alternative *cis* [2424] conformer is of higher energy due to *trans*-annular H$\cdots$H interactions (Krotz, Kuo & Barton, 1993); donor atoms are all directed to the same side, but do not deviate sufficiently from planarity for ideal *cis*-octahedral coordination; the [48] is more suitable and more flexible. The short *trans*-annular H$\cdots$H contacts at 2.1 Å in the molecular mechanics minimized structure cause a distortion from ideal $C_{2v}$ to $C_2$ symmetry. The anangular $C_{2v}$ *cis* conformer (up–down–up–down donor atoms) reverted to the $D_{2d}$ anangular conformer with 139° (CSCC) and 73° (SCCS) torsion angles when molecular mechanics minimization was attempted (Fig. 3).

The macrocycle in $Cl_3Bi(1b)$, VOSTEC, has a distorted [2343] conformation and one donor atom is significantly further (3.21 Å) from the Bi centre than the other three (mean 3.02 Å). The variant with ideal $C_s$ symmetry is slightly higher in energy than the distorted $C_1$ geometry in which van der Waals repulsion between two *trans*-annular H atoms is reduced slightly. {The $C_s$ conformer is more stable for (1*a*), but significantly higher in energy than the [3333]*B* or [48] since the short 'side' requires short *trans*-angular and *exo* hydrogen contacts and was not observed in the data set.} KUNMEL displays $\eta^2$-coordination of [2334]*A* (1*b*) to a $PdCl_2$ moiety, differing from the [2334]*B* conformation in that one of the *anti* torsion angles is about a C—C rather than a C—S bond. Molecular mechanics calculations suggest that the free ligand has a higher energy than the [3333]*B* conformer, however, non-bonded repulsions between the Cl ligands and uncoordinated thioether donors in KUNMEL are probably lower in [2334]*A*.

## 5. Conclusions

This study has shown that it is possible to classify successfully the conformations of both free and metal-coordinated unsaturated 12-membered oxa and thia macrocycles, using symmetry-modified Jarvis–Patrick clustering, and to present the results in conformational space by means of principal component analysis plots. For the oxa macrocycles the plots show that the [3333] and [66] conformations are both common for the free ligands; if the macrocycle is engaged in hydrogen-bonding this determines the conformation, although the [66] conformation, whose energy is predicted to be slightly lower from molecular mechanics calculations, is usually adopted in the absence of such interactions. There is a significant change in the conformational populations for macrocycles coordinated to a metal ion. With metals that favour square planar, square-based pyramidal, seven-coordinate 4:3 or square anti-prismatic geometries the [3333] conformation dominates, whilst for metals with a *cis*-octahedral ligand arrangement the macrocycles adopt a [48] in preference to the [66] configuration, the latter not being observed in any *endo*-dentate coordination complex.

For the thia macrocycles there are insufficient examples for a complete analysis; however, it is clear that the conformations adopted by the free ligands, with the sulfur lone pairs directed away from the interior of the macrocycle, are not suited to coordination to a metal ion and substantial conformational reorganization is required before chelation can occur. These chelating conformations are, however, similar to those adopted by the oxa ligands. This difference in behaviour between the oxa and thia macrocycles can be rationalized in terms of the differing torsion-angle preferences for C$X$CC and $X$CC$X$ units ($X$ = O, S), depending on the conformational requirements of the lone pairs and dative lone pairs on the O and S atoms.

These observed conformational differences, obtained using all the appropriate structures in the CSD, are mirrored by the predicted low-energy structural forms calculated for the free ligands using molecular mechanics methods. Furthermore, they show which of the metal-coordinated conformations have the lower energies, by analogy to their frequency of occurrence, without having to consider the problems associated with including metal-atom parameters in the molecular mechanics calculations.

## References

Allen, F. H. & Fortier, S. (1993). *Acta Cryst.* B**49**, 1021–1031.

Allen, F. H. & Taylor, R. (1991). *Acta Cryst.* B**47**, 404–412.

Allen, F. H., Davies, J. E., Galloy, J. J., Johnson, O., Kennard, O., Macrae C. F., Mitchell, E. M., Mitchell, G. F., Smith, J. M. & Watson, D. G. (1991). *J. Chem. Inf. Comp. Sci.* **31**, 187–204.

Allen, F. H., Doyle, M. J. & Auf der Heyde, T. P. E. (1991). *Acta Cryst.* B**47**, 412–424.

Allen, F. H., Doyle, M. J. & Taylor, R. (1991*a*). *Acta Cryst.* B**47**, 29–40.

Allen, F. H., Doyle, M. J. & Taylor, R. (1991*b*). *Acta Cryst.* B**47**, 41–49.

Allen, F. H., Doyle, M. J. & Taylor, R. (1991*c*). *Acta Cryst.* B**47**, 50–61.

Allen, F. H., Howard, J. A. K & Pitchford, N. A. (1993). *Acta Cryst.* B**49**, 910–928.

Allinger, N. L. (1977). *J. Am. Chem. Soc.* **99**, 8127–8134.

Allinger, N. L. & Yuh, Y. H. (1981). *QCPE. Bulletin of the Chemistry Program Exchange.* Department of Chemistry, Indiana University, Bloomington, Indiana, USA.

Auf der Heyde, T. P. E. (1990). *J. Chem. Educ.* **67**, 461–469.

Batchelor, R. J., Einstein, F. W. B., Gay, I. D., Gu, J.-H. & Pinto, B. M. (1991). *J. Organomet. Chem.* **411**, 147–157.

Beech, J., Cragg, P. J. & Drew, M. G. B. (1994). *J. Chem. Soc. Dalton Trans.* pp. 719–729.

Blake, A. J. & Schröder, M. (1990). *Adv. Inorg. Chem.* **35**, 2–80.

Blake, A. J., Gould, R. O., Halcrow, M. A., Schröder, M. (1993). *Acta Cryst.* B**49**, 773–779.

Blaschette, A., Nagel, K.-H. & Jones, P. G. (1994). *Z. Naturforsch. Teil B*, **49**, 36–42.

Boer, F. P., Neuman, M. A., van Remoortere, F. P. & Steiner, E. C. (1974). *Inorg. Chem.* **13**, 2826–2834.

Bovill, M. J., Chadwick, D. J., Sutherland, I. O. & Watkin, D. (1980). *J. Chem. Soc. Perkin Trans. II*, pp. 1529–1543.

Cambridge Structural Database (1992). *CSD User's Manual.* Cambridge Crystallographic Data Centre, 12 Union Road, Cambridge, England.

Cambridge Structural Database (1994). *CSD User's Manual.* Cambridge Crystallographic Data Centre, 12 Union Road, Cambridge, England.

Cambridge Structural Database (1995). *CSD User's Manual.* Cambridge Crystallographic Data Centre, 12 Union Road, Cambridge, England.

Chatfield, C. & Collins, A. J. (1980). *Introduction to Multivariate Analysis.* London: Chapman and Hall.

Columbia University (1994). *MacroModel Interactive Molecular Modeling System.* Version 4.5. Department of Chemistry, Columbia University, New York, USA.

Cooper, S. R. (1988). *Acc. Chem. Res.* **21**, 141–146.

Cram, D. J. (1988). *Angew. Chem. Int. Ed. Engl.* **27**, 1009–1120.

Dale, J. (1963). *J. Chem. Soc.* pp. 93–111.

Dale, J. (1973). *Acta Chem. Scand.* **27**, 1115–1129.

Desper, J. M., Powell, D. R. & Gellman, S. H. (1990). *J. Am. Chem. Soc.* **112**, 4321–4324.

Dunitz, J. D. & Shearer, H. M. M. (1960). *Helv. Chim. Acta*, **43**, 18–35.

Fausto, R., Teixeira-Dias, J. J. C. & Carey, P. R. (1987). *J. Mol. Struct.* **159**, 137–152.

Fyles, T. M. & Gandour, R. D. (1992). *J. Incl. Phenom.* **12**, 3291–3298.

Groth, P. (1978). *Acta Chem. Scand. Ser. A*, **32**, 279–280.

Hancock, R. D. (1990). *Acc. Chem. Res.* **23**, 253–257.

Hay, B. P., Rustad, J. R. & Hostetler, C. J. (1993). *J. Am. Chem. Soc.* **115**, 11158–11164.

Jarvis, R. A. & Patrick, E. A. (1973). *IEEE Trans. Comput.* **22**, 1025–1034.

Juaristi, E. (1979). *J. Chem. Educ.* **56**, 438–441.

Krotz, A. H., Kuo, L. Y. & Barton, J. K. (1993). *Inorg. Chem.* **32**, 5963–5974.

Lehn, J.-M. (1988). *Angew. Chem. Int. Ed. Engl.* **27**, 90–112.

Lindoy, L. F. (1989). *The Chemistry of Macrocyclic Ligand Complexes.* Cambridge University Press.

Lockhart, J. C., Mousley, D. P., Stuart Hill, M. N., Tomkinson, N. P., Teixidor, F., Almajano, M. P., Escriche, L., Casabo, F. J., Sillanpää, R. & Kivekäs, R. (1992). *J. Chem. Soc. Dalton Trans.* pp. 2889–2897.

Marsh, R. E. (1986). *Acta Cryst.* B**42**, 193–198.

McDowell, R. S. (1965). *J. Mol. Spectrosc.* **17**, 365–367.

Mohamadi, F., Richards, N. G. J., Guida, W. C., Liskamp, R., Lipton, M., Caufield, C., Chang, G., Hendrickson, T. & Still, W. C. (1990). *J. Comput. Chem.* **11**, 440–467.

Murray-Rust, P. & Bland, R. (1978). *Acta Cryst.* B**34**, 2527–2533.

Murray-Rust, P. & Raftery, J. (1985*a*). *J. Mol. Graph.* **3**, 50–59.

Murray-Rust, P. & Raftery, J. (1985*b*). *J. Mol. Graph.* **3**, 60–69.

Pedersen, C. J. (1988). *Angew. Chem. Int. Ed. Engl.* **27**, 1021–1027.

Pett, V. B., Diaddario, L. L., Dockal, E. R., Corfield, P. W., Ceccarelli, C., Glick, M. D., Ochrymowycz, L. A. & Rorabacher, D. B. (1983). *Inorg. Chem.* **22**, 3661–3670.

Podo, F., Némethy, G., Indovina, P. L., Radics, L. & Viti, V. (1974). *Mol. Phys.* **27**, 521–559.

Remoortere, F. P. van & Boer, F. P. (1974). *Inorg. Chem.* **13**, 2071–2078.

Remoortere, F. P. van, Boer, F. P. & Steiner, E. C. (1975). *Acta Cryst.* B**31**, 1420–1426.

Robinson, G. H. & Sangokoya, S. A. (1988). *J. Am. Chem. Soc.* **110**, 1494–1497.

Rogers, R. D. & Kurihara, L. K. (1986). *Inorg. Chim. Acta*, **116**, 171–177.

Rogers, R. D., Rollins, A. N. & Benning, M. M. (1988). *Inorg. Chem.* **27**, 3826–3835.

Samuel, G. & Weiss, R. (1969). *Tetrahedron Lett.* pp. 2803–2806.

Setzer, W. N., Tang, Y., Grant, G. J. & Van Derveer, D. G. (1991). *Inorg. Chem.* **30**, 3652–3656.

Uiterwijk, J. W. H. M., Harkema, S., van de Waal, B. W., Göbel, F. & Nibbeling, H. T. M. (1983). *J. Chem. Soc. Perkin Trans. 2*, pp. 1843–1855.

Watzky, M. A., Waknine, D., Heeg, M. J., Endicott, J. F. & Ochrymowyzc, L. A. (1993). *Inorg. Chem.* **32**, 4882–4888.

Willey, G. R., Lakin, M. T. & Alcock, N. W. (1992). *J. Chem. Soc. Dalton Trans.* pp. 591–596.

Wolf, R. E. Jr, Hartman, J. R., Storey, J. M. E, Foxman, B. M. & Cooper, S. R. (1987). *J. Am. Chem. Soc.* **109**, 4328–4335.

Zefirov, N. S. (1977). *Tetrahedron*, **33**, 3193–3202.